DNA Computing

DOI: 10.1002/anie.201202356

Reconfigurable Three-Dimensional DNA Nanostructures for the Construction of Intracellular Logic Sensors**

*Hao Pei, Le Liang, Guangbao Yao, Jiang Li, Qing Huang, and Chunhai Fan**

Molecular logic gates hold great potential for multi-parameter sensing, intelligent diagnostics, and molecular computation.[1] DNA-based logic gates[2] and computation[3] are particularly interesting because of their self-assembly and the recognition ability of DNA. Several systems have been demonstrated by exploiting these properties of DNA, such as the trainable molecular-automation (MAYA) series,[4] DNA digital circuits solving square-root problems,[5] and autonomous brain-like systems.[6] Among many applications, in vivo logic gates have proven particularly useful for therapeutic applications.[7] It is important to have intelligent drug-delivery systems that are programmable to have a time-variable rate of delivery or deliver drugs in response to environmental stimuli at the site of injection.[8] Hence, an ideal DNA logic-gate system for medical purposes would have high cell permeability, design generality, and robust stability in biological fluids.

The emergence of DNA nanotechnology offers great opportunities for such applications.[9] Turberfield and coworkers and our group have shown that three-dimensional (3D) DNA tetrahedral nanostructures[10] can easily enter live cells and release carried drugs.[11] We thus predict that the incorporation of DNA tetrahedra into DNA computing might provide a generic platform for developing intelligent systems that can function in vivo to simultaneously detect disease markers and control cargo release to selectively kill cancer cells. Toward this goal, we developed DNA tetrahedra that show programmed configuration switching in response to external stimuli. By adapting a series of DNA structures (i-motif,[12] anti-ATP aptamer (AAA),[13] T-rich mercury-specific oligonucleotide (MSO),[14] and hairpin structures) to DNA tetrahedra (Scheme 1), we constructed AND, OR, XOR, and INH logic gates, as well as a half-adder operation. In addition, we also demonstrated the use of DNA logic gates for intracellular detection of ATP in living cells.

3D DNA nanostructure-based logic gates are constructed by using a series of DNA tetrahedra that are responsive to various targets, given that such dynamic structures embedded with hairpin loops are reconfigurable.[15] DNA tetrahedra were assembled with four different DNA sequences using a simple annealing method. Each edge of the tetrahedron contains a nick site that is positioned in the middle of the edge strands. By adding dynamic sequences (i-motif, AAA, and MSO) into the complementary strand opposite the nick site on one or two of the edges, the configuration of the tetrahedron can change in response to the input of specific targets (such as, protons, ATP, and mercury ions). Native polyacrylamide gel electrophoresis (PAGE) analysis confirmed the assembly of these reconfigurable DNA tetrahedra (see Supporting Information, Figure S3–8). These dynamic sequences stay in a "floppy" ssDNA conformation in the absence of their target molecule but change to a "rigid" conformation after binding to the target, which turns the tetrahedra from a relaxed (R-) state to a taut (T-) state. To provide an output signal for such an R-to-T transition, we attached a Forster resonance energy-transfer (FRET) pair (a rhodamine green (RG) fluorophore and a DABCYL (D) quencher) on either side of the nick site. Since FRET is dependent on distance changes between the donor (fluorophore) and acceptor (quencher), the target-induced configuration changes of the DNA tetrahedra are translated into variation of the fluorescence intensity. Notably, the fluorescent quantum yield of RG is insensitive to pH variations in the range of pH 4.0–9.0, which ensures that the fluorescence change depends only on the conformational change of the DNA tetrahedra.[12]

We initially designed an INH operation by using a reconfigurable tetrahedron with one edge containing a dynamic i-motif sequence (Figure 1a). In a solution pH 5.0, the cytosine (C) bases in the i-motif sequence were protonated and folded

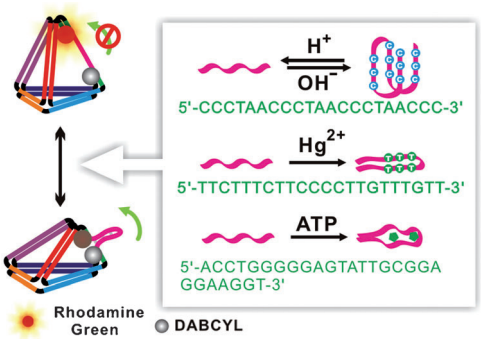

Scheme 1. Scheme of DNA tetrahedra that are reconfigurable by adapting dynamic sequences in one arm (i-motif, AAA, and MSO). Green arrow = FRET signal.

[*] H. Pei,[+] L. Liang,[+] G. Yao, Dr. J. Li, Prof. Q. Huang, Prof. C. Fan
Laboratory of Physical Biology, Shanghai Institute of Applied Physics, Chinese Academy of Sciences
Shanghai 201800 (China)
E-mail: fchh@sinap.ac.cn

[+] These authors contributed equally to this work.

[**] This work was Supported by the National Basic Research Program of China (973 program, 2012CB932600), NSFC (21105028, 21075128, 90913014, 31100716, and 61008056), CAS (KJCX2-EW-N03).

Supporting information for this article (experimental details) is available on the WWW under http://dx.doi.org/10.1002/anie.201202356.

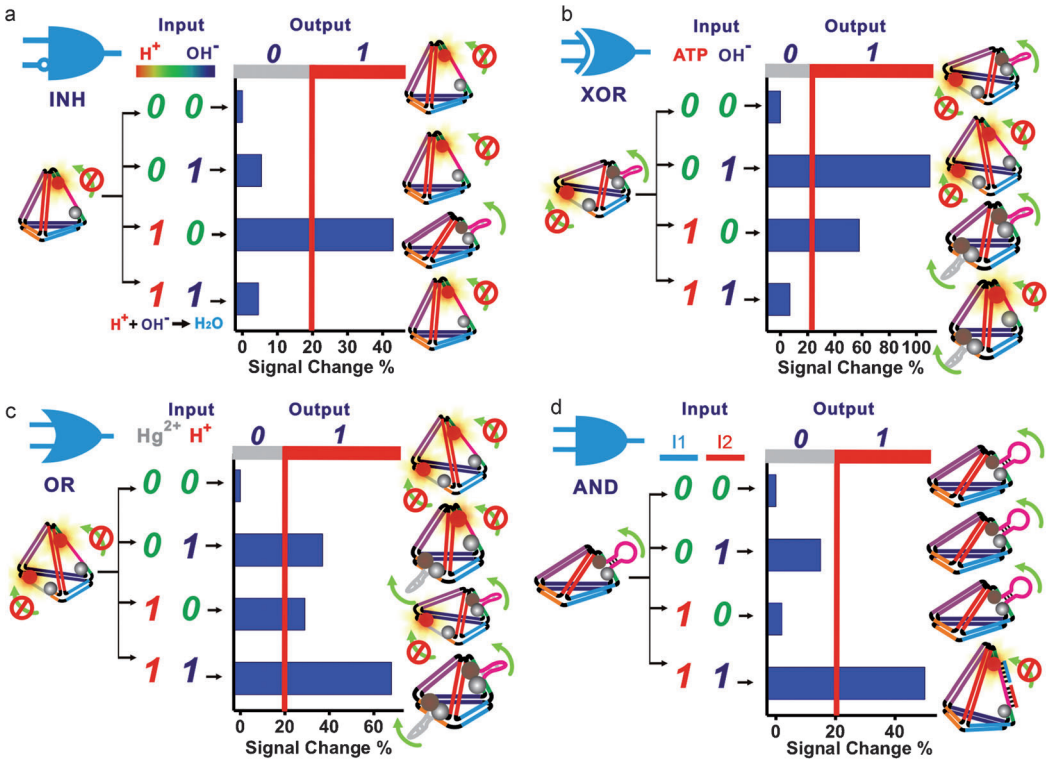

Figure 1. Logic operations (INH, XOR, OR, and AND) using 3D DNA tetrahedra. a) INH logic gate using P-tetra with H^+ and OH^- ions as inputs. b) XOR logic gate using PA-tetra with ATP and OH^- ions as inputs. c) OR logic gate using PM-tetra with Hg^{2+} and H^+ ions as inputs. d) AND logic gate using H-tetra with two partially complementary DNA strands (I1, I2) as inputs. The output of each operation is measured as a change in fluorescence signal.

into the compact, rigid i-motif structure (T-state), which held the D in close proximity to the RG and quenched the fluorescence. When the pH value of the solution was raised to 8.0, the i-motif structure disassembled and stretched owing to the tensile force in the DNA tetrahedron (R-state), which separated D and RG and turned on the fluorescence. A pH titration experiment revealed that the fluorescence of RG was indeed strongly dependent on solution pH (Supporting Information, Figure S1). We found an "S"-shaped titration curve, with the sharpest transition in the range from pH 6.0–7.0 and two plateaus beyond that range. The transition point at pH 6.3 was consistent with a previously reported value ($pK_a = 6.3$).[16]

The logic of an INH gate is that the output is "1" only when one particular input is applied. Based on the above results, this proton responsive tetrahedron (P-tetra) could be used as an INH gate by using the addition of H^+ and OH^- ions as the inputs, and the change in fluorescence as the output (Figure 1a). P-tetra in a solution of pH 7.0 was set as the initial state of this INH gate, where the tetrahedron is in the R-state. The addition of either H^+ or OH^- ions (3 mM) was defined as the "on" or "1" state, and the "off" or "0" state corresponded to no addition of ions. The output was defined based on the variation of the fluorescence intensity of RG, with "1" for a variation greater than ±20% (either increase or decrease). When the appropriate amount of H^+ ions were introduced to the system (input = 1), the pH value of the solution decreased from 7.0 to 6.0, which fell within the transition range, the C residues were protonated within the tetrahedron, resulting in the switch of the tetrahedron from the R-state to the T-state and the turn-on of the fluorescence (signal variation = 44%, output = 1). When OH^- ions (input = 1) were introduced, the pH shifted from 7.0 to 8.0, which fell within the plateau region in the titration curve and did not lead to significant conformational change of the tetrahedron (signal variation = 5%, output = 0). When the both inputs (H^+ and OH^- ions) were set at either "1" or "0" (input = 1/1 or 0/0), the solution pH value did not change because of acid–base neutralization and the tetrahedron remained in the R-state (signal change = 0% or 5%; output = 0). Therefore, the output was "1" only upon the addition of H^+ (input = 1/0), while it was "0" for all other inputs (0/0, 1/0, 1/1; Figure 1a), corresponding to an INH gate.

XOR and OR gates were constructed using tetrahedra with two edges containing dynamic sequences (Figure 1b,c). An XOR gate means that the output is "1" only if one of the inputs, but not both, is applied. We designed a tetrahedron with two dynamic sequences (i-motif and AAA) incorporated into opposite edges (PA-tetra, Figure 1c). The RG and D FRET pair was used in both dynamic sequences. The initial state of the tetrahedron was set to a conformation with the AAA-containing edge stretched (in the absence of ATP) and the i-motif-containing edge contracted (pH 5.0). Additions of either ATP or OH^- were defined as the "on" or "1" states of the input, and the output definition was the same as that of the INH gate. As shown in Figure 1b, the addition of 3 mM OH^- ions (input = 0/1) resulted in a change in pH value from 5.0 to 7.0, unfolded the i-motif structure, and increased the fluorescence intensity (signal variation = 110%, output = 1); introduction of ATP molecules (1 mM, input = 1/0) folded the AAA into a rigid tertiary structure, leading to the contraction of the AAA sequence and a decrease in the fluorescence intensity (signal variation = 58%, output = 1). However, when both OH^- ions and ATP were added to the system (input = 1/1), the stretch of the i-motif sequence counteracted

the contraction of the AAA sequence, resulting in minimal net variation of the fluorescence intensity (signal variation = 7%, output = 0). Therefore, it was possible to construct an XOR gate with two dynamic sequences, with little interference between one another. In an XOR operation with the PA-tetra, the output was "1" when either ATP or OH^- ions were added (input = 1/0 or 0/1), however when both ATP and OH^- ions were added simultaneously (input = 1/1), the output became "0".

A similar strategy was used to construct an OR gate from a tetrahedron with two opposite edges containing a dynamic proton-responsive i-motif and a mercury-responsive MSO sequence (PM-tetra; Figure 1c). In the initial state of the PM-tetra, both edges were stretched (pH 7.0 and no Hg^{2+} ions). Hence, the addition of either H^+ or Hg^{2+} ions, or both (input = 1/0, 0/1 or 1/1), caused the folding of one or two sequences and decreased the fluorescence intensity (output = 1). The output was "0" only when neither input was applied (Figure 1c).

We also constructed an AND gate using a tetrahedron with one edge containing a hairpin sequence (H-tetra, Figure 1d). Initially, the complementary stem of the hairpin held the structure in the T-state, then the cooperative hybridization of two partially complementary strands of DNA (I1 and I2) turned it into a stretched duplex. Notably, I1 and I2 were designed such that either of them was only partially complementary to the hairpin and could not open it alone. Hence, like in a typical AND operation, the output was "1" only when both I1 and I2 were added into the system (input = 1/1), and it was "0" when only one of the I1/I2 strands or neither was added (input = 1/0, 0/1; Figure 1d).

It is noteworthy that the starting condition decides the type of gate. For example, the XOR gate shown in Figure 1b has a starting condition of compact-relaxed. We could, in principle, turn it into an OR gate (shown in Figure 1C) by using starting conditions of either relaxed-relaxed or compact-compact. It is thus possible to use one tetrahedral structure to realize multiple logic operations.

It is expected that the integration of these logic gates could lead to more complex operations (e.g., molecular circuits). To examine this idea, we constructed a DNA tetrahedra-based molecular half-adder (HA) circuit by using an XOR and an AND gate (Figure 2), which could perform partial binary integer addition. The output from the XOR gate corresponded to the sum bit for the addition, while the output from the AND gate represented the carry bit. We combined the XOR-input-1 (ATP) and the AND-input-1 (I1) to form the HA-input-1, and similarly the XOR-input-2 (OH^- ions) and the AND-input-2 (I2) to afford the HA-input-2. We expected to obtain distinct output signals when identical inputs were applied to both gates. Indeed, when only one of the HA inputs was added to the half-adder individually, we observed high signal change (> 20%, output = 1) for the sum bit, while low signal change (< 20%, output = 0) for the carry bit, equaling the decimal number 1 (Figure 2). Alternatively, when both HA inputs were added to the half-adder circuit, the signal change was reversed (carry bit = 1, sum bit = 0), equaling the decimal number 2. While such logic operations with DNA tetrahedra are still simple and preliminary, we

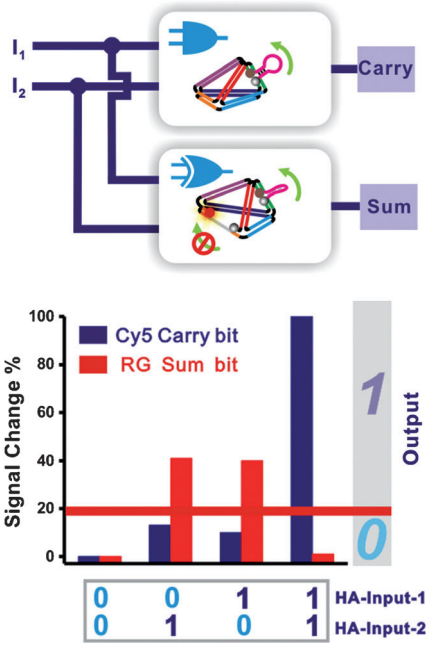

Figure 2. Scheme (top) and signal output (bottom) of a 3D DNA tetrahedron-based molecular half-adder (HA) circuit with the combination of an XOR and an AND gate. The output from the XOR gate corresponds to the sum bit for the addition, while the output from the AND gate represents the carry bit. When only one HA input is present, the output is "1" for the sum bit, while the carry bit is "0". When both HA inputs are present, the output is inverted, which forms the binary half-adder arithmetic operation.

expect that much more complex logic computations can be made using more elaborate DNA nanostructures created by DNA origami technology.[17]

Besides their computation applications, these scaffolded DNA tetrahedra provide a means to directly detect molecular targets,[18] a property that is useful for both in vitro and in vivo diagnostics. As a proof-of-concept, we developed tetrahedra-based biosensors[19] for a small molecule (ATP) and a metal ion (Hg^{2+}). The tetrahedron containing AAA on one edge (A-tetra) sensitively responded to the presence of ATP. The fluorescence variation showed a non-linear dependence on ATP concentration in the range of 2–600 μM, with a detection limit of 2 μM (Figure 3a,b). Control experiments revealed that analogue molecules of ATP, for example, cytidine triphosphate (CTP), guanosine triphosphate (GTP), and uridine triphosphate (UTP), only led to weak responses, suggesting the high selectivity of this tetrahedral biosensor (Figure 3c). Similarly, a Hg^{2+}-responsive DNA tetrahedron with one edge containing the MSO sequence (M-tetra) was used to detect Hg^{2+} ions. M-tetra could sensitively detect mercury down to 20 nM Hg^{2+} ions, and showed high discrimination against 11 different metal ions (all of 1 μM; Figure 3d–f).

Having established the signaling capability of the scaffolded DNA tetrahedra, we further investigated whether such nanostructures could function in cells for intracellular detection. We designed a tetrahedral nanostructure that is responsive to ATP in living cells (using HeLa cells as a model). The A-tetra was modified with Cy3 (donor) and Cy5 (acceptor) fluorophores at either termini of the nick site, instead of RG

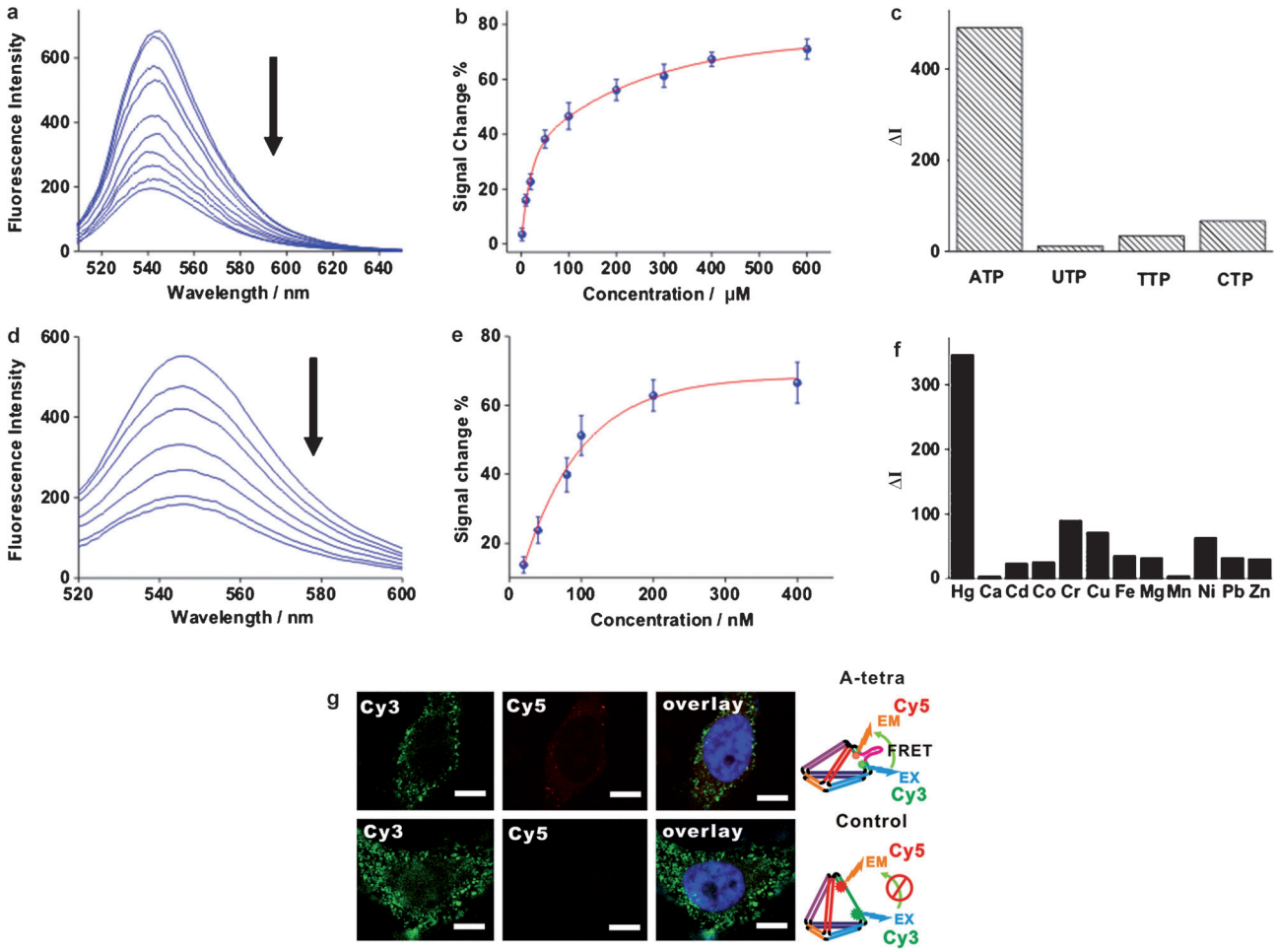

Figure 3. a) Fluorescent spectra of A-tetra upon addition of ATP (0, 2, 10, 20, 50, 100, 200, 300, 400, or 600 μM). b) Calibration curve for various concentrations of ATP. c) Selectivity of the A-tetra based ATP sensor over UTP, TTP, and CTP (all 1 mM). d) Fluorescent spectra of M-tetra upon addition of Hg^{2+} (0, 20, 40, 80, 100, 200, or 400 nM). e) Calibration curve for various concentrations of Hg^{2+} ions. f) Selectivity of the M-tetra based Hg^{2+} sensor over different metal ions (all 1 μM). g) Detection of intracellular ATP in living cells using A-tetra (labeled with a Cy3 and Cy5 FRET pair). Scale bar = 20 μm.

and D labels, for imaging in live cells. As a control, an M-tetra was prepared that was not responsive to the ATP concentration. HeLa cells were incubated with the DNA tetrahedra, and imaged using scanning confocal fluorescence microscopy. Nuclear staining with DAPI (Figure 3g) and flow cytometry (Supporting Information, Figure S10) studies showed that these nanostructures predominantly remained in the cytoplasm. Cells treated with A-tetra showed much greater intensity of Cy5 fluorescence (red) and lesser intensity of Cy3 fluorescence (green) than those with the M-tetra (Figure 3g), indicating that intracellular ATP brought the two dyes in A-tetra together, enabling efficient FRET from Cy3 to Cy5. Such ATP-induced increase of Cy5 fluorescence and decrease of Cy3 fluorescence was consistent with the in vitro experiments in aqueous solution (Supporting Information, Figure S2). Also importantly, these cellular imaging studies clearly showed that DNA tetrahedra nanostructures were cell permeable[11] and could potentially function as logic gates inside the cell.

In summary, we have constructed various scaffolded logic gates (INH, XOR, AND, OR, and half-adder) by using a series of reconfigurable DNA tetrahedra nanostructures containing dynamic sequences that are responsive to protons, metal ions (Hg^{2+}), small molecules (ATP), and complementary DNA strands. These 3D DNA nanostructure-based computing components provide several unprecedented advantages that make them a promising method for biosensing and genetic control in vivo. First, these reconfigurable DNA tetrahedra nanostructures can be rapidly and reliably synthesized with high yields,[10a] providing a readily available scaffold for the construction of molecular logic gates and sensors. Second, the rigid, stable, tetrahedral architecture of the nanostructures provides a uniform scaffold for the incorporation of a wide range of dynamic sequences, and the shape change of the DNA tetrahedron can be precisely predicted.[15] Third, since these DNA tetrahedra-based computing components are essentially of biological origin, it is possible to apply these logic operations to in vivo sensing and therapy.[20] The high cell permeability and stability of DNA tetrahedra nanostructures[11] and controllable shape of these DNA cages offers a new opportunity to "logically" control drug release in cells. Finally, by immobilizing these DNA

tetrahedra on surfaces,[19a] it could improve the function of DNA motors for constructing complicated surface-based smart devices,[21] owing to their rigid and stable architecture. Given these advantages, we expect these 3D DNA tetrahedra could become a highly generic and versatile structure for the development of DNA nanotechnology and DNA computers that function both in vitro and in vivo.

Received: March 26, 2012
Revised: June 22, 2012
Published online: August 7, 2012

Keywords: biosensors · DNA computing · DNA structures · logic gates

[1] a) R. Baron, O. Lioubashevski, E. Katz, T. Niazov, I. Willner, *Angew. Chem.* **2006**, *118*, 1602 – 1606; *Angew. Chem. Int. Ed.* **2006**, *45*, 1572 – 1576; b) A. P. de Silva, S. Uchiyama, *Nat. Nanotechnol.* **2007**, *2*, 399 – 410; c) Z. Q. Guo, W. H. Zhu, L. J. Shen, H. Tian, *Angew. Chem.* **2007**, *119*, 5645 – 5649; *Angew. Chem. Int. Ed.* **2007**, *46*, 5549 – 5553; d) D. H. Qu, Q. C. Wang, H. Tian, *Angew. Chem.* **2005**, *117*, 5430 – 5433; *Angew. Chem. Int. Ed.* **2005**, *44*, 5296 – 5299.

[2] a) A. Saghatelian, N. H. Volcker, K. M. Guckian, V. S. Y. Lin, M. R. Ghadiri, *J. Am. Chem. Soc.* **2003**, *125*, 346 – 347; b) B. Shlyahovsky, Y. Li, O. Lioubashevski, J. Elbaz, I. Willner, *ACS Nano* **2009**, *3*, 1831 – 1843; c) M. N. Stojanovic, T. E. Mitchell, D. Stefanovic, *J. Am. Chem. Soc.* **2002**, *124*, 3555 – 3561.

[3] a) J. Elbaz, O. Lioubashevski, F. A. Wang, F. Remacle, R. D. Levine, I. Willner, *Nat. Nanotechnol.* **2010**, *5*, 417 – 422; b) G. Seelig, D. Soloveichik, D. Y. Zhang, E. Winfree, *Science* **2006**, *314*, 1585 – 1588.

[4] a) R. J. Pei, E. Matamoros, M. H. Liu, D. Stefanovic, M. N. Stojanovic, *Nat. Nanotechnol.* **2010**, *5*, 773 – 777; b) M. N. Stojanovic, D. Stefanovic, *Nat. Biotechnol.* **2003**, *21*, 1069 – 1074.

[5] L. L. Qian, E. Winfree, *Science* **2011**, *332*, 1196 – 1201.

[6] L. L. Qian, E. Winfree, J. Bruck, *Nature* **2011**, *475*, 368 – 372.

[7] a) Y. Benenson, B. Gil, U. Ben-Dor, R. Adar, E. Shapiro, *Nature* **2004**, *429*, 423 – 429; b) M. Leisner, L. Bleris, J. Lohmueller, Z. Xie, Y. Benenson, *Nat. Nanotechnol.* **2010**, *5*, 666 – 670; c) K. Rinaudo, L. Bleris, R. Maddamsetti, S. Subramanian, R. Weiss, Y. Benenson, *Nat. Biotechnol.* **2007**, *25*, 795 – 801; d) E. Shapiro, B. Gil, *Science* **2008**, *322*, 387 – 388; e) Z. Xie, L. Wroblewska, L. Prochazka, R. Weiss, Y. Benenson, *Science* **2011**, *333*, 1307 – 1311; f) C. J. Delebecque, A. B. Lindner, P. A. Silver, F. A. Aldaye, *Science* **2011**, *333*, 470 – 474; g) B. Gil, M. Kahan-Hanum, N. Skirtenko, R. Adar, E. Shapiro, *Nano Lett.* **2011**, *11*, 2989 – 2996.

[8] R. Langer, D. A. Tirrell, *Nature* **2004**, *428*, 487 – 492.

[9] a) N. C. Seeman, *Nature* **2003**, *421*, 427 – 431; b) A. V. Pinheiro, D. R. Han, W. M. Shih, H. Yan, *Nat. Nanotechnol.* **2011**, *6*, 763 – 772; c) Y. He, T. Ye, M. Su, C. Zhang, A. E. Ribbe, W. Jiang, C. D. Mao, *Nature* **2008**, *452*, 198 – 201; d) Y. Krishnan, F. C. Simmel, *Angew. Chem.* **2011**, *123*, 3180 – 3215; *Angew. Chem. Int. Ed.* **2011**, *50*, 3124 – 3156; e) F. C. Simmel, *Nanomedicine* **2007**, *2*, 817 – 830; f) E. S. Andersen, M. Dong, M. M. Nielsen, K. Jahn, R. Subramani, W. Mamdouh, M. M. Golas, B. Sander, H. Stark, C. L. P. Oliveira, J. S. Pedersen, V. Birkedal, F. Besenbacher, K. V. Gothelf, J. Kjems, *Nature* **2009**, *459*, 73 – 75; g) H. Liu, D. S. Liu, *Chem. Commun.* **2009**, 2625 – 2636; h) J. W. Liu, Z. H. Cao, Y. Lu, *Chem. Rev.* **2009**, *109*, 1948 – 1998; i) Y. Xing, Z. Yang, D. Liu, *Angew. Chem.* **2011**, *123*, 12140 – 12142; *Angew. Chem. Int. Ed.* **2011**, *50*, 11934 – 11936.

[10] a) R. P. Goodman, I. A. T. Schaap, C. F. Tardin, C. M. Erben, R. M. Berry, C. F. Schmidt, A. J. Turberfield, *Science* **2005**, *310*, 1661 – 1665; b) R. P. Goodman, R. M. Berry, A. J. Turberfield, *Chem. Commun.* **2004**, 1372 – 1373.

[11] a) J. Li, H. Pei, B. Zhu, L. Liang, M. Wei, Y. He, N. Chen, D. Li, Q. Huang, C. H. Fan, *ACS Nano* **2011**, *5*, 8783 – 8789; b) A. S. Walsh, H. F. Yin, C. M. Erben, M. J. A. Wood, A. J. Turberfield, *ACS Nano* **2011**, *5*, 5427 – 5432.

[12] D. S. Liu, S. Balasubramanian, *Angew. Chem.* **2003**, *115*, 5912 – 5914; *Angew. Chem. Int. Ed.* **2003**, *42*, 5734 – 5736.

[13] T. Hermann, D. J. Patel, *Science* **2000**, *287*, 820 – 825.

[14] A. Ono, H. Togashi, *Angew. Chem.* **2004**, *116*, 4400 – 4402; *Angew. Chem. Int. Ed.* **2004**, *43*, 4300 – 4302.

[15] R. P. Goodman, M. Heilemann, S. Doose, C. M. Erben, A. N. Kapanidis, A. J. Turberfield, *Nat. Nanotechnol.* **2008**, *3*, 93 – 96.

[16] J. L. Leroy, K. Gehring, A. Kettani, M. Gueron, *Biochemistry* **1993**, *32*, 6019 – 6031.

[17] P. W. K. Rothemund, *Nature* **2006**, *440*, 297 – 302.

[18] Z. L. Zhang, Y. Q. Wen, Y. Ma, J. Luo, L. Jiang, Y. L. Song, *Chem. Commun.* **2011**, *47*, 7407 – 7409.

[19] a) H. Pei, N. Lu, Y. L. Wen, S. P. Song, Y. Liu, H. Yan, C. H. Fan, *Adv. Mater.* **2010**, *22*, 4754 – 4758; b) H. Pei, Y. Wan, J. Li, H. Y. Hu, Y. Su, Q. Huang, C. H. Fan, *Chem. Commun.* **2011**, *47*, 6254 – 6256; c) Y. L. Wen, H. Pei, Y. Wan, Y. Su, Q. Huang, S. P. Song, C. H. Fan, *Anal. Chem.* **2011**, *83*, 7418 – 7423.

[20] a) S. Modi, M. G. Swetha, D. Goswami, G. D. Gupta, S. Mayor, Y. Krishnan, *Nat. Nanotechnol.* **2009**, *4*, 325 – 330; b) S. M. Douglas, I. Bachelet, G. M. Church, *Science* **2012**, *335*, 831 – 834.

[21] D. Liu, E. Cheng, Z. Yang, *NPG Asia Mater.* **2011**, *3*, 109 – 114.

